Prediction of Potentially Unstable Electrical Activity during Embryonic Development of Rodent Ventricular Myocytes

Chikako Okubo[1,3], Hitomi Sano[1,3], Yasuhiro Naito[1,2,3], Masaru Tomita[1,2,3]

[1]Institute for Advanced Biosciences, Keio University, Kanagawa, Japan
[2]Systems Biology Program, Graduate School of Media and Governance, Keio University, Kanagawa, Japan
[3]Department of Environment and Information Studies, Keio University, Kanagawa, Japan

Abstract

In order to evaluate developmental changes in embryonic ventricular cells at early embryonic (EE) and late embryonic (LE) stage, we aimed to predict potentially unstable action potentials (APs) that could be lethal to developing ventricular cells. Two models of the Kyoto and the Luo-Rudy model were used for simulation of 512 representative combinations by switching the relative activities of 9 ionic components whose activities vary between the EE and LE stages. Out of these 512 combinations in Kyoto model, 144 combinations were predicted potentially unstable resulting from combinations of funny current (I_f), inward rectifier current (I_{K1}), sustained inward current (I_{st}), L-type Ca^{2+} current (I_{CaL}), and Na^+ current (I_{Na}). Other 208 and 160 combinations were predicted quiescent membrane potentials and regular spontaneous APs. Based on these results, we suggest that sequential switches of the relative activities of I_{Na}, I_f, and I_{K1} enable cells to avoid unstable patterns.

1. Introduction

In rodent, the electrophysiological properties of individual ion channels have been investigated in isolated ventricular myocytes at the representative 4 stages, early embryonic (EE), late embryonic (LE), neonatal, and adult, via patch clamp methods [1-3]. In EE stage, spontaneous action potentials (APs) have been reported, eventually disappearing in passive contracting cell in the LE stage [4]. In addition to regular spontaneous APs, irregular and unstable APs have been reported in single mouse embryonic myocytes [5]. Although the existence of such irregular activities in single cells has been reported at the representative stages, potentially unstable activities must also be identified between the stages along with the mechanisms behind such activities to elucidate the entire course of development of the heart.

Jonsson *et al*. (2012) combined molecular biology and computer simulation to demonstrate that human embryonic stem cell-derived cardiomyocytes (hESC-CM) have an immature electrophysiological phenotype [6]. Thus, computer simulation is a powerful approach for confirming experimental data and providing insight into possible functional mechanisms of heart development.

2. Methods

We utilized the two mathematical models, the Kyoto and Luo-Rudy model, in which the relative activities of ionic components were switched independently between EE and LE stages to represent different combinations of the components in embryonic guinea pig ventricular cells.

2.1. Embryonic ventricular cell models

Previously, we simulated the APs of rodent ventricular cells at the EE, LE stages using the Kyoto model, an electrophysiological model of guinea pig ventricular cells [7]. Briefly, quantitative changes in various ionic components were represented as the activities of the components in developmental stages relative to that in the adult stage. These relative activities were multiplied by corresponding conductance (pA/mV) or conversion factors (pA/pF·mM) in common sets of mathematical equations. We adopted the same procedure in the present study and the updated Kyoto model [8].

2.2. Switching stages of ionic components

We selected the 9 components to be switched between the EE and LE stages: funny current (I_f), sustained inward current (I_{st}), inward rectifier current (I_{K1}), Na^+ current (I_{Na}), L-type Ca^{2+} current (I_{CaL}), Na^+/Ca^{2+} exchange

current (I_{NaCa}), transient outward current (I_{to}), ATP-sensitive K^+ current (I_{KATP}), and a set of 4 electrical components of the SR. All 4 components located in the SR, the Ca^{2+} release through the RyR channel in the SR (I_{RyR}), Ca^{2+} leak from the SR ($I_{SR,leak}$), the SR Ca^{2+} pump (I_{SRCA}), and Ca^{2+} transfer from the SR uptake site to the release site ($I_{SR,transfer}$), develop along with development of the SR and were treated as a set of components in the SR. The other ionic components in the model were assumed to have constant current densities during embryonic development. Table 1 show the relative activity values of the 9 components relative to adult model. We assumed that the 9 components switched relative activities directly from EE to LE values without intermediate levels, independently from the other components.

Table 1. The relative activities for the early embryonic (EE) and late embryonic (LE) stages.

Ionic currents	EE	LE
I_{Na}	0.07	1.0
I_{CaL}	0.46	0.78
I_f	1.0	0.0
I_{st}	1.0	0.0
I_{K1}	0.11	1.0
I_{KATP}	0.32	0.88
I_{to}	0.11	0.27
I_{NaCa}	4.95	1.74
SR-related components	0.04	0.3

2.3. Computer simulation procedure

We simulated 512 (2^9) combinations of intact EE models for 600 s, switching the relative activities of the 9 components between EE and LE values. For those combinations that showed no spontaneous activity for 600 s, we applied external stimulation at 2.5 and 1.0 Hz to determine whether the intact cells functioned as contracting cells. We further verified our predictions by simulations with the 32 (2^5) combinations of the Luo-Rudy model [9]. The relative activities of I_{Na}, I_f, I_{K1}, I_{CaL}, and SR-related components were switched between EE and LE values. Although the original Luo-Rudy model does not contain I_f, we implemented a mathematical model for I_f [10]. The other components, I_{to}, I_{KATP}, I_{st}, and I_{NaCa}, were not considered.

3. Results

We predicted unstable membrane excitation patterns from computer simulation of 512 combinations and identified I_{Na}, I_f, I_{K1}, I_{CaL}, and I_{st}, as components potentially responsible to avoid the predicted unstable patterns.

3.1. Classification of the 512 combinations

In the 512 combinations of simulation using the Kyoto model, 208 combinations were predicted to have positive resting membrane potential (RMP) >-80 mV. We observed 160 regular spontaneous APs and 144 potentially unstable APs. Because the values of I_{KATP}, I_{to}, I_{NaCa}, and SR-related components did not significantly influence the results, we focused on the remaining 5 pivotal currents, I_{Na}, I_f, I_{K1}, I_{st}, and I_{CaL} (Fig. 1).

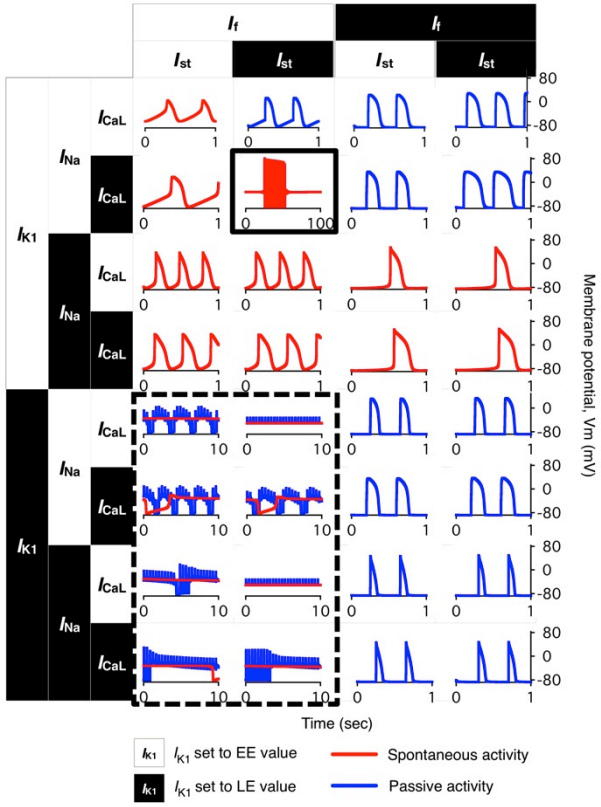

Figure 1. Simulated membrane potentials of 32 representative combinations switching activity values for 5 components. Potentially unstable combinations are highlighted with solid and dashed boxes.

3.2. Potentially unstable patterns

128 combinations out of 512 were predicted to have 2 RMPs, at -35 mV and under -60 mV, when the relative activity of I_{K1} was set to the LE value and that of I_f was set to the EE value, regardless of the other three components (Fig. 1, dashed box and Fig. 2a). The membrane potential was depolarized when the Ca^{2+}-activated background cation current (I_{LLCa}), which is activated when the intracellular Ca^{2+} concentration ($[Ca^{2+}]_i$) is high (Fig. 2a).

In 16 combinations, burst-like APs were observed when the relative activities of I_{CaL} and I_{st} were set to the LE values while those of I_{Na}, I_f, and I_{K1} were set to the EE values (Fig. 1, solid box). Figure 2b show the interval

between the bursts was approximately 70 s at -50 mV. As the repetitive bursts were terminated, the Na^+/K^+ pump current (I_{NaK}) became dominant, and I_{NaK} gradually decreased during the quiescent state between the bursts. These combinations failed to produce normal APs in response to application of external stimulus.

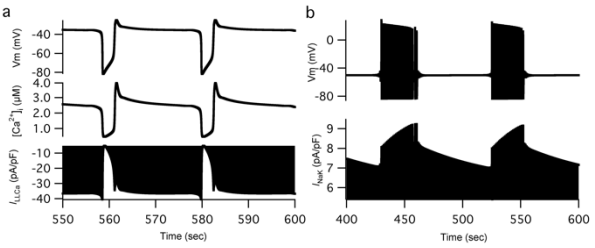

Figure 2. (a) Observed two resting membrane potentials and (b) burst-like action potentials (APs).

3.3. Simulation with external stimulus

We applied an external stimulus to produce APs in resting cell models with no spontaneous electrical activity, and paced them for 600 s. The amplitude of hSL at high frequency (2.5 Hz) was slightly smaller than that at low frequency (1.0 Hz) when the relative activities of I_f and I_{K1} were set to the LE values and those of the other components fixed to the EE values (Fig. 3a). On the other hand, when the relative activity of I_{Na} was switched to the LE value in addition to those of I_f and I_{K1}, the amplitude of hSL was twice as large with stimulus at 2.5 Hz than at 1.0 Hz.

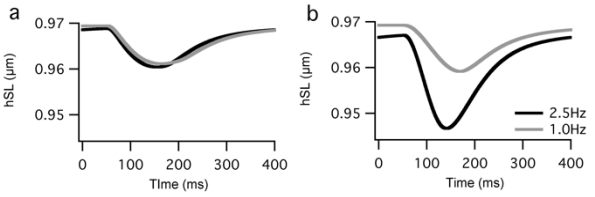

Figure 3. The half sarcomere lengths of the combinations that I_{Na} switched to the EE and LE values.

The peak $[Ca^{2+}]_i$ was larger in models with the relative activity of I_{Na} switched to the LE value (0.29 μM) than in models with I_{Na} fixed to the EE value (0.10 μM) when the models were externally stimulated at 2.5 Hz. The difference resulted from larger Ca^{2+} influx via I_{NaCa} and Ca^{2+} release from the SR. In addition, we observed a subtle decrease in resting intercellular Na^+ concentrations ($[Na^+]_i$) from the LE (2.30 mM) to the adult (2.22 mM) models, and $[Na^+]_i$ was even higher when the relative activities of I_{Na}, I_f, and I_{K1} were switched to the LE from the EE model (2.33 mM). $[Na^+]_i$ was relatively low, however, when only the relative activities of I_f and I_{K1} were switched to the LE from the EE model (1.46 mM).

3.4. Sequential changes in I_{Na}, I_f, and I_{K1}

Figure 5 shows changes in the APs and accompanying ionic currents as we sequentially switched I_{Na}, I_f, and I_{K1} from the EE model; spontaneous APs disappeared when I_{Na}, I_f, and I_{K1} were all switched to LE values, although AP was inducible by external stimulus. The maximum diastolic potential (MDP) gradually shifted in the negative direction and the overshoot potential became larger as I_{Na} increased, followed by disappearance of I_f (Table 2). The basic cycle length (BCL) of the model with I_{Na} switched to the LE value was shortest (0.34 ms) among the three spontaneous APs; the BCL was originally 0.51 ms in the EE model with disappearance of I_f. The peak amplitude of I_{CaL} decreased from -100 pA to -10 pA and that of I_{Na} increased from 0 pA to -5000 pA, and I_{Na} became responsible for rapid depolarization rather than I_{CaL}.

Table 2. MDP and BCL of spontaneous action potentials

	EE model	I_{Na} set to LE	I_{Na} and I_f set to LE
MDP (mV)	-81.40	-82.48	-84.73
BCL (sec)	0.51	0.34	0.78

4. Discussion

We suggest that I_{CaL} and I_{st} should not be switched before increase in I_{Na}, and showed that the sequential switch in I_{Na}, I_f, and I_{K1} could avoid unstable patterns.

4.1. Required order of I_f and I_{K1}

To avoid unstable patterns with 2 RMPs (Fig. 2a), we determined that I_{K1} should increase before disappearance of I_f. Abnormally high $[Ca^{2+}]_i$ was observed when I_{K1} increased approximately 10-fold (from 0.11 to 1.0) before disappearance of I_f (from 1.0 to 0.0). Because of the abnormally high $[Ca^{2+}]_i$, we designated these combinations as unstable patterns, and suggest that I_f should disappear before I_{K1} increases to avoid unstable patterns with 2 RMPs. I_f is known to be a pacemaker current and plays an important role in spontaneous firing of APs in 9.5-days post coitum (dpc) mice, but decreases by 80% by 18 dpc [5]. In contrast, the current density of I_{K1} is very small in 12-dpc rats, and increases nearly 10-fold by the end of embryonic development, contributing to a negative shift in RMP [11].

Moreover, 8 of the 32 combinations in the Luo-Rudy model failed to produce APs despite application of external stimulus when the relative activity of I_f was set to the LE values and those of all the other components were set at the EE values (data not shown). These 8 combinations in Luo-Rudy model were among the combinations that defined unstable patterns in the Kyoto model with 2 RMPs. However, the 2 RMPs were not

observed in the Luo-Rudy model.

4.2. An early increase in I_{Na}

We observed burst-like membrane potentials (Fig. 2b) when I_{CaL} increased and I_{st} disappeared simultaneously before I_{Na} increased. We suggest that combinations that showed burst-like activities should be avoided during embryonic development, because such activities in the pulmonary vein are known to cause atrial fibrillation [12]. Therefore, I_{Na} should increase to the LE level at the beginning of embryonic development, because an increase in I_{Na} was also related to stronger shortening force at 2.5 Hz than at 1.0 Hz (Fig. 3). In addition, $[Na^+]_i$ was higher in combinations in which the relative activities of I_{Na}, I_f, and I_{K1} were set to the LE values (2.33 mM) and in the LE model (2.30 mM) vs. the adult model (2.22 mM) in their resting states. These results are consistent with a report that $[Na^+]_i$ in EE ventricles was higher than in more developed embryos, while $[K^+]_i$ remained constant throughout embryonic development in the chick [13].

4.3. Sequential switches of I_{Na}, I_f, and I_{K1}

Figure 4 demonstrated that sequential switching of I_{Na}, I_f, and I_{K1} could avoid unstable patterns. This change in the dependence of depolarization from the Ca^{2+} current to the Na^+ current is consistent with experimental observations in rodent ventricular myocytes [14] in which MDP shifted in a negative direction, also consistent with our simulation (Table 2). On the other hand, the BCL shortened when I_{Na} increased and lengthened when I_f disappeared (Fig. 4), although EE hearts have a large range of heart rates, 61–219 min^{-1} in 11.5-dpc rats [15], and the beating rhythm of EE ventricular cells is generally slow and irregular [16].

5. Conclusion

In the Kyoto and Luo-Rudy models, our simulation results suggested that I_f *d*should disappear before the 10-fold increase in I_{K1} to avoid potentially unstable patterns. Of the 9 components switched between EE and LE levels in the Kyoto model, combinations of switches in I_{Na}, I_{CaL}, I_f, I_{st}, and I_{K1} densities were responsible for potentially unstable patterns.

References

[1] Kato Y, Masumiya H, Agata N, Tanaka H, Shigenobu K. Developmental changes in action potential and membrane currents in fetal, neonatal and adult guinea-pig ventricular myocytes. J Mol Cell Cardiol 1996;28(7):1515-1522.

[2] Davies MP, An RH, Doevendans P, Kubalak S, Chien KR, Kass RS. Developmental changes in ionic channel activity in the embryonic murine heart. Circ Res 1996;78(1):15-25.

[3] Tohse N, Seki S, Kobayashi T, Tsutsuura M, Nagashima M, Yamada Y. Development of excitation-contraction coupling in cardiomyocytes. Jpn J Physiol 2004;54(1):1-6.

[4] Yokoshiki H, Tohse N. Developmental changes of ion channels. In: Kurati Y, Terzic A, Cohen MV, Sperelakis N. Heart physiology and pathophysiology. New York: Academic Press, 2001;719-35.

[5] Yasui K, Liu W, Opthof T, Kada K, Lee JK, Kamiya K, Kodama I. I(f) current and spontaneous activity in mouse embryonic ventricular myocytes. Circ Res 2001;88(5):536-542.

[6] Jonsson MK, Vos MA, Mirams GR, Duker G, Sartipy P, de Boer TP, van Veen TA. Application of human stem cell-derived cardiomyocytes in safety pharmacology requires caution beyond hERG. J Mol Cell Cardiol 2012;52(5):998-1008.

[7] Itoh H, Naito Y, Tomita M. Simulation of developmental changes in action potentials with ventricular cell models. Syst Synth Biol 2007;1(1):11-23.

[8] Kuzumoto M, Takeuchi A, Nakai H, Oka C, Noma A, Matsuoka S. Simulation analysis of intracellular Na+ and Cl- homeostasis during beta 1-adrenergic stimulation of cardiac myocyte. Prog Biophys Mol Biol 2008;96(1-3):171-186.

[9] Faber GM, Rudy Y. Action potential and contractility changes in [Na(+)](i) overloaded cardiac myocytes: a simulation study. Biophys J 2000;78(5):2392-2404.

[10] Kurata Y, Matsuda H, Hisatome I, Shibamoto T. Effects of pacemaker currents on creation and modulation of human ventricular pacemaker: theoretical study with application to biological pacemaker engineering. Am J Physiol Heart Circ Physiol 2007;292(1):701-718.

[11] Masuda H, Sperelakis N. Inwardly rectifying potassium current in rat fetal and neonatal ventricular cardiomyocytes. Am J Physiol 1993;265:1107-1111.

[12] de Bakker JM, Ho SY, Hocini M. Basic and clinical electrophysiology of pulmonary vein ectopy. Cardiovasc Res 2002;54(2):287-294.

[13] Klein RL High Na content of early embryonic chick heart. Am J Physiol 1963;205(2):370.

[14] DeHaan RL, Fujii S, Satin J. Cell interactions in cardiac development. Develop Growth Differ 1990;32(2):233-241.

[15] Couch JR, West TC, Hoff HE. Development of the action potential of the prenatal rat heart. Circ Res 1969;24(1):19-31.

[16] Nagashima M, Tohse N, Kimura K, Yamada Y, Fujii N, Yabu H. Alternation of inwardly rectifying background K+ channel during development of rat fetal cardiomyocytes. J Mol Cell Cardiol 2001;33(3):533-543.

Address for correspondence.

Yasuhiro Naito
5322 Endo Fujisawa, Kanagawa, Japan
E-mail: ynaito@sfc.keio.ac.jp